

## The ITER ECH FS Upper Launcher mm-wave Design based on a Synergy Study with the Equatorial Launcher

*M.A. Henderson<sup>1</sup>, R. Chavan<sup>1</sup>, R. Bertizzolo<sup>1</sup>, A Bruschi<sup>2</sup>, D. Campbell<sup>3</sup>, E Ciattaglia<sup>3</sup>, S Cirant<sup>2</sup>, I Danilov<sup>4</sup>, F. Dolizy<sup>1</sup>, D. Farina<sup>2</sup>, R Heidinger<sup>4</sup>, K Kleefeldt<sup>4</sup>, J.-D. Landis<sup>1</sup>, A. Moro<sup>2</sup>, E. Poli<sup>5</sup>, G. Ramponi<sup>2</sup>, G. Saibene<sup>3</sup>, O. Sauter<sup>1</sup>, A Serikov<sup>4</sup>, H. Shidara<sup>1</sup>, P. Spaeh<sup>4</sup>, V.S. Udintsev<sup>1</sup>, H. Zohm<sup>5</sup>, C. Zucca<sup>1</sup>*

First Author e-mail: [mark.henderson@epfl.ch](mailto:mark.henderson@epfl.ch)

**1** CRPP, EURATOM – Confédération Suisse, EPFL, CH-1015 Lausanne Switzerland. **2** Istituto di Fisica del Plasma, EURATOM-ENEA-CNR Association, 20125 Milano, Italy. **3** EFDA Close Support Unit, Boltzmannstrasse 2, D-85748 Garching, Germany. **4** Forschungszentrum Karlsruhe, EURATOM-FZK, D-76021 Karlsruhe, Germany. **5** IPP-Garching, Max Planck-Institute für Plasmaphysik, D-85748 Garching, Germany

**Abstract.** The ITER ECH heating and current drive system consists of 24 MW (20 MW delivered) at 170GHz, which can be directed to either the equatorial (EL) or upper (UL) port launching antennas (launchers) depending on the desired physics application. The UL reference design uses a front steering (FS) mirror that sweeps the beam in a poloidal plane providing co-ECCD over the outer third of the plasma cross section. A novel frictionless, backlash-free steering mechanism has been developed for an increased reliability. The design avoids components such as bearings and push-pull rods, which tend to grip in conventional launchers in use on present day ECH systems. Flexure pivots replace bearings and a pneumatic seal-less actuator using pressurised helium integrated into the rotating mirror assembly offers a fast and precise response avoiding push-pull rods, linkages representing sliding bearings and remote actuators. The result is a complete self-contained frictionless kinematic assembly rotating the steering mirror up to  $\pm 7^\circ$  ( $\pm 14^\circ$  for RF beam).

The launcher has a single dedicated purpose of stabilising the neoclassical tearing modes (NTM), with the launcher steering range accessing the region in which the  $q=3/2$  or 2 flux surfaces are expected for scenarios susceptible to NTMs. The performance of the FS launcher far exceeds (by a factor of 1.5 to 3) that required by the physics to stabilize the NTM. The two mirror (focusing and steering) system of the FS launcher essentially decouples the steering and focusing functions of the launcher, offering the flexibility to increase the access range beyond that required by the NTM stabilisation such that the launcher can access further inward for sawteeth control. Extending the range of the UL can relax the EL steering range, which can then be optimised for enhanced performance for improved central deposition and potentially for counter ECCD.

**1. Introduction.** The Electron Cyclotron Heating and Current Drive (ECH&CD) system<sup>1</sup> for ITER is planned to consist of 24MW (60 min) installed power at 170GHz and an additional 3MW (~3sec) at ~120GHz for assisting in plasma breakdown. The layout of the ECH&CD system is shown in figure 1a, which consists of 24 170GHz gyrotrons ( $\geq 1\text{MW}$ ), 3 ~120GHz gyrotrons, associated power supplies (not shown), evacuated 63.5mm HE<sub>11</sub> waveguide (~100m in length) and two launching systems: one Equatorial Launcher (EL) or four Upper Launchers (UL). The ECH power can be directed to either launcher during a discharge with the choice depending on the physics application. For example, when desiring more central deposition ( $0.0 \leq \rho_{\psi} \leq 0.65$ ) the EL is used, while for off axis deposition ( $0.64 \leq \rho_{\psi} \leq 0.93$ ) the UL is used so that ECH&CD can be deposited across nearly the entire plasma cross section. The reference design of both launchers uses a front steering (FS) mirror placed close to the plasma offering the largest steering range and optimized beam focusing. The EL<sup>2</sup> (see figure 1c) has three sets of steering mirrors with 8 beams incident on each mirror and steered in a horizontal plane over the range of  $20^\circ \leq \beta \leq 45^\circ$ , where  $\beta$  is the beam's toroidal angle measured from a poloidal plane to the beam centre line. The UL (see figure 1b) has two steering mirrors per port plug with 4 beams incident on each mirror. The beams are steered in a vertical plane over a range of  $\Delta\alpha \sim 22^\circ$  (values of  $\alpha$  are different for the two steering mirrors), where  $\alpha$  corresponds to the angle from a horizontal plane down to the projected beam centre on to a poloidal plane. The vertical steering plane has  $\beta \sim 20^\circ$  relative to a poloidal plane, this toroidal injection angle offers the largest peak  $j_{\text{CD}}$  for a maximum stabilisation efficiency<sup>3</sup> of the neoclassical tearing mode (NTM)<sup>3</sup>.

The upper launcher reference design had used the remote steering (RS) concept<sup>4</sup>, which has the steering mechanism located outside of the torus vacuum. This concept offers reduced complexity in the repair and maintenance of the steering mechanism, but limits the physics performance. Designs using both the RS<sup>5</sup> and FS<sup>6</sup> were developed (along with their integration into the port plug<sup>7</sup>) under the

European Fusion Development Agreement (EFDA) with both designs presented to ITER-IT for evaluation at the end of 2005<sup>8</sup>. ITER-IT selected the FS design as the reference design based on its higher physics performance, reduced costs and sufficient operating reliability and safety. A set of critical design issues (CDI) for the FS launcher were identified and solutions to these issues were provided to ITER to help in evaluating the compatibility of the FS launcher to the ITER environment. A general review of the critical design issues of the FS launcher is given in the following section. One significant difference between the two launcher designs was the physics performance, the FS launcher achieved higher physics performance and offered an extension of the potential physics applications capable of being achieved from the UL and would relax the demands placed on the EL. A synergetic launcher design is proposed that partitions the physics applications based on the capabilities (or strengths) of each launcher, this is outlined and compared with the present system in chapter 3.

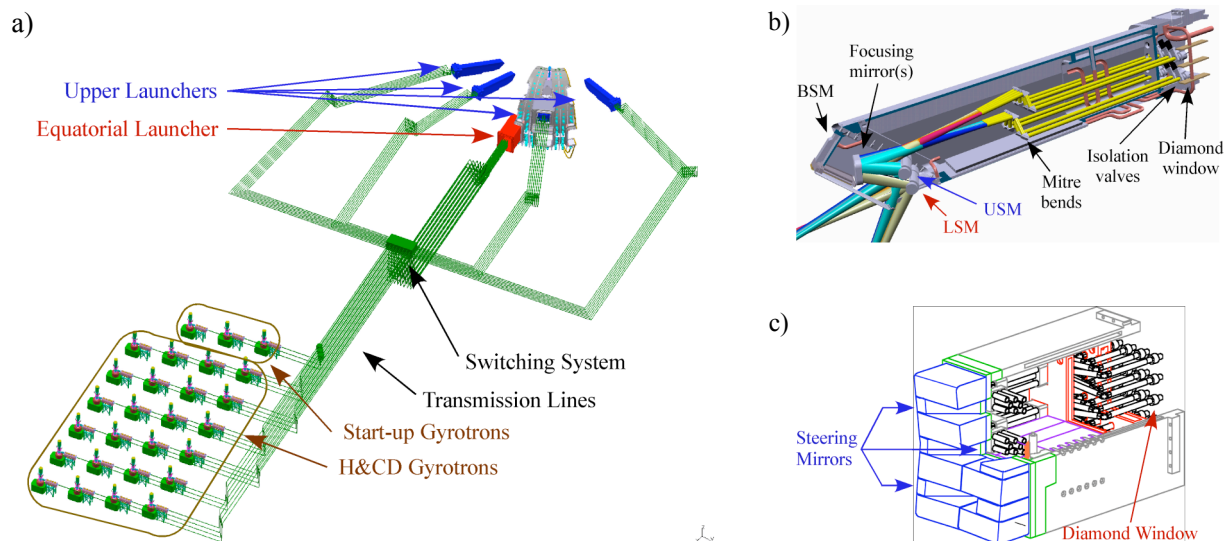


**FIGURE 1.** a) Layout of the 24MW ECH system for ITER. b) UL<sup>6</sup> has 8 beams per port (4 ports in total). All beams have a fixed toroidal injection angle ( $\beta \sim 20^\circ$ ) and are scanned in a poloidal plane with  $\Delta\alpha \sim \pm 11^\circ$ . c) EL<sup>2</sup> has all 24 beams in one port with all beams scanned in a toroidal plane over the range of  $20^\circ \leq \beta \leq 45^\circ$ .

**2. FS launcher design.** A simplified view of the current FS launcher design is shown in Figure 1b. Eight circular HE<sub>11</sub> waveguides ( $\phi_{WG}=63.5\text{mm}$ , similar to the waveguide used in the transmission line) enter the port plug entrance on the right, with a diamond window and an in-line gate or isolation valve placed in each waveguide prior to the closure plate with the waveguides arranged in two rows of four. The isolation valve is on the plasma side of the diamond window, such that the window can be isolated for leak testing or repair. A miter bend ‘dog-leg’ assembly is used to angle the 8 beams (both in toroidal and poloidal directions) to one (or two) focusing mirror(s) with the incident beams partially overlap in both toroidal and poloidal directions. The reflected beams are then directed downward to two separate flat steering mirrors, which redirect the beams into the plasma with a toroidal injection angle of  $\beta \approx 20^\circ$ . Since the beams are allowed to expand from the waveguide aperture, they can be refocused to a narrow waist ( $\sim 21\text{mm}$ ) far into the plasma ( $> 1.6\text{ m}$  after steering mirror). The angular rotation of the steering mirror provides access along the resonance layer from  $Z_{res} = 1.8$  to  $3.6\text{m}$ , corresponding to  $0.64 \leq \rho_p \leq 0.93$ . Overlapping the beams on the mirrors permits a larger beam for a finite focusing mirror size within the confined space of the blanket shield module (BSM). Note that the space in the BSM is shared between the mm-wave components and shield blocks to protect the components and port plug from the neutron flux. The focusing mirror curvature, waveguide tilt angle and relative orientation of the steering mechanism have been optimized to insure that the 4 beams are deposited nearly coincident in the plasma.

**2.1 Critical design issues** The majority of components used in the FS launcher design are similar to components that are available commercially, with the main exception being the steering mechanism ensemble. A new innovative design of the steering mechanism<sup>9,10</sup> (see Figure 2a) is being developed that provides rotation of the steering mirror based on the compliant deformation of

structural components offering a frictionless and backlash free mechanical movements and avoiding the invessel tribological difficulties inherent in present day FS systems. Traditional ball bearings are replaced with elastically compliant flexure pivots and the movement is controlled using an integrated gaseous helium pneumatic actuator system working against preloaded compressive springs in place of the push-pull rods. This eliminates the components that typically grip in present day FS launchers offering an improved reliability and precision in controlling the steering mirror angle. The bellows are pressurized from the outside, as shown in Figure 5b, which offers a more stable configuration avoiding the squirm instability when the bellows are internally pressurised as illustrated in Figure 5c. A pair of coiled cooling pipes with either a single or double wall provides a flexible coolant feed to the mirror, following a similar design to that proposed for the EL<sup>2</sup>.

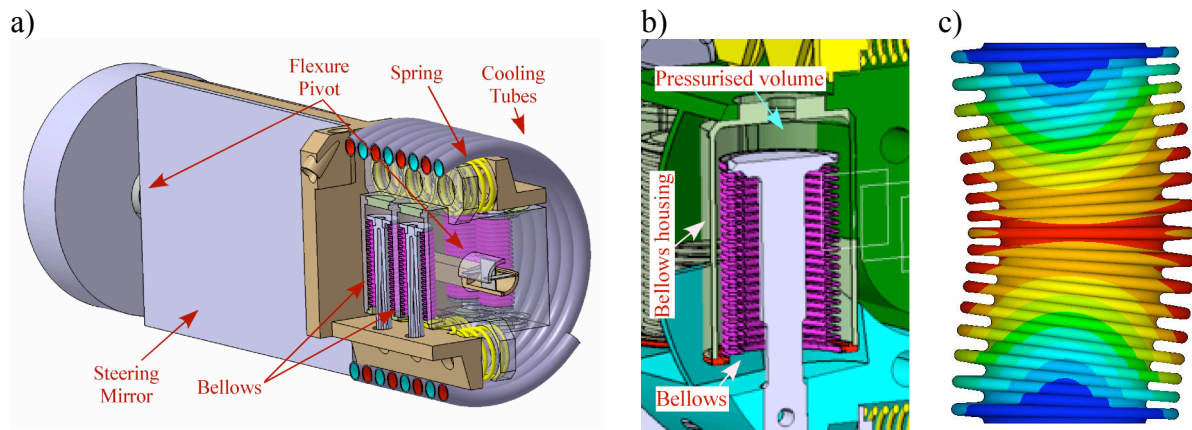


**Figure 2** a) The steering mechanism design with the critical components identified, b) a zoomed in view of the bellows in an externally pressurised configuration similar to combustion engine piston and c) the squirm instability simulated in an internally pressurised bellows.

The reliable operation of the steering mechanism for the duration of the ITER operating lifetime has been demonstrated based on analytical, finite element modelling (FEM) and/or accepted international standards (for example EJMA<sup>11</sup> in the case of the bellows) for all of the critical components forming the steering mechanism ensemble. The CDI document was assembled with the aim of identifying each critical issue and then providing solution(s) to each issue. The CDI divided the critical issues into four groups as shown in Table 1. A brief description of an example issue(s) in each category is described below.

<b>Table 1: The four categories of the critical design issues associated with the FS launcher.</b>		
<b>N</b>	<b>CDI</b>	<b>Description</b>
5	General Design	General design of the steering mirror, mechanism and actuator along with steps for a fail-safe system
7	Induced EM forces	Design steps to accommodate Electro-Magnetic forces arising from induced currents during a vertical disruption event
6	Cyclic Fatigue	Estimation of the number of cycles to failure of the bellows, springs, flexure pivots and spiral cooling lines taking into account irradiation effects.
6	Thermal effects	Description of the cooling techniques used to evacuate the heat deposited in the mm-wave components from the RF beams and nuclear heating.

**General Design** One issue that was strongly emphasised was the concept of a ‘fail-safe’ design. If a component failed it had to be isolated to allow continued operation of ITER with a minimal interruption to the plasma operation. One example of a fail-safe design is the cooling and pneumatic actuators of the steering mechanism. Both cooling and pneumatic circuits are separated into dedicated lines isolated from other systems in the port plug. If a leak occurs in one circuit, then that circuit can be closed off and evacuated to limit the intrusion of either the gas or coolant to the torus. Note that active cooling of the components is not required with no mm-wave load, the nuclear heating is evacuated via thermal conduction and radiation.

The same valve system can be used to isolate each circuit and perform periodic leak checks to insure that the vacuum integrity of the flexible cooling lines and actuator bellows are maintained. An

additional example of a fail-safe design is the diamond window, which has the isolation valve placed on the plasma side. If the window breaks, then the valve can be closed isolating the window from the torus vacuum. Repair of the window can then be made without affecting the torus volume. Also, pumping access between the valve and window permits leak testing of the window in-situ to insure that the tritium boundary is maintained.

**Induced EM Forces** The induced currents in the steering mirror coupled with the background magnetic field results in large torques in the steering mirror of  $\sim 500\text{Nm}$  during a vertical disruption event (VDE). This torque is translated to a force on the flexure pivot of  $\sim 1.4\text{kN}$  perpendicular to the axis of rotation, which may buckle the thin fins. The fins are dimensioned to avoid such buckling and withstand up to  $10^3$  VDEs at the worst rotation angle based on analytical and finite element modelling (see Figure 3a), while maintaining adequate flexibility needed for rotating the steering mirror. To avoid halo currents from flowing through the assembly the steering mirror ensemble is designed to have only a single grounding contact to the port structure.

**Cyclic Fatigue** The steering mechanism ensemble is designed to operate during the full lifetime of ITER (20 years) prior to encountering cyclic fatigue. The launcher is required to stabilise the NTMs that will occur on either the  $q=2$  or  $3/2$  magnetic surfaces for the three scenarios<sup>12</sup> 2, 3a and 5. This entails that during a discharge an NTM can occur on either surface and that the launcher will have to redirect the EC deposition from one surface to the other, referred to as an NTM switching cycle. In addition, any given flux surface will move during a discharge as a result of variations in the plasma parameters, which corresponds to a smaller modulation of deposition location. An estimated 21'000 NTM cycles and 840'000 modulation cycles are expected to occur during the ITER lifetime assuming 70% of the discharges experience NTMs with an average plasma pulse length of 400s. The component that will first be susceptible to fatigue will be the bellows, with the number of cycles to fatigue depending on the total rotation of the steering mechanism as shown in figure 3b (note that the total rotation is twice that of an NTM cycle and the fatigue includes radiation effects). The present steering mechanism is required to rotate  $\pm 6.5^\circ$  (mechanical design of  $\pm 7^\circ$ ), which sustains  $>50'000$  full cycles (twice the NTM cycle) prior to the onset of cyclic fatigue based on the EJMA standards.

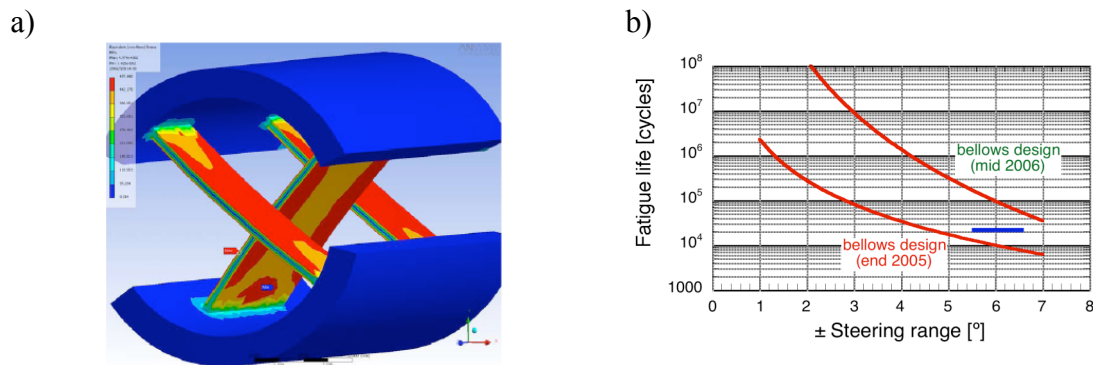


**Figure 3** a) Stresses induced in the flexure pivot during a VDE simulated using ANSYS and b) cyclic fatigue curves as a function of steering range for the bellows design at the end of 2005 (nickel bellows) and mid 2006 (Inconel 718), the blue line represents the cycle requirements for the UL.

**Thermal Effects** There are two sources that heat up the mm-wave components: the RF beam incident on the mirror surfaces and the plasma (thermal and nuclear radiation). The RF absorption creates the highest power densities, which depends on the injected power (assumed 2.0 MW per beam), surface roughness (between 1.3 and 2.0), mirror material (Cu), mirror temperature and beam profile. The optics of the launcher is designed for large spot size on the free space mirrors ( $>50\text{mm}$ , so that the beam can be focused to a small spot size far into the plasma), which results in low power density ( $\leq 2.0\text{MW/m}^2$ ) such power densities can easily be evacuated by relatively simple cooling channels in the mirror body. The power density on the mitre bend mirror is much larger since the beam is relatively small (equivalent to a beam spot size of  $\sim 20\text{mm}$ ), resulting in a peak power density of  $\sim 3.6\text{MW/m}^2$ . The resulting peak temperature is  $\leq 200^\circ\text{C}$  using non-optimised cooling channels, see the ANSYS FEM shown in Figure 4a.



The plasma as a heat source has two contributions: thermal (for components in a line of sight with the plasma) and nuclear radiation (volumetric heating from gamma and neutron radiation). The sum total only contributes a minor heat load relative to the RF absorption with radiated power levels of  $<0.2\text{MW/m}^2$  for plasma facing components and nuclear volumetric heating of the order of  $\leq 1\text{MW/m}^3$ . The later complicates the design of the steering mechanism components such as the bellows and springs, which have poor thermal conductivity due to the long path lengths to regions of active cooling. The cooling efficiency is increased by relying on a combination of conduction and radiation. For example, the bellows housing will be actively cooled at  $\leq 120^\circ\text{C}$ , the absorbed power in the bellows will then radiate to this surface, with the maximum temperature reaching  $<190^\circ\text{C}$  as shown in the ANSYS FEM of Figure 4b, compatible with the bellows operating temperature.

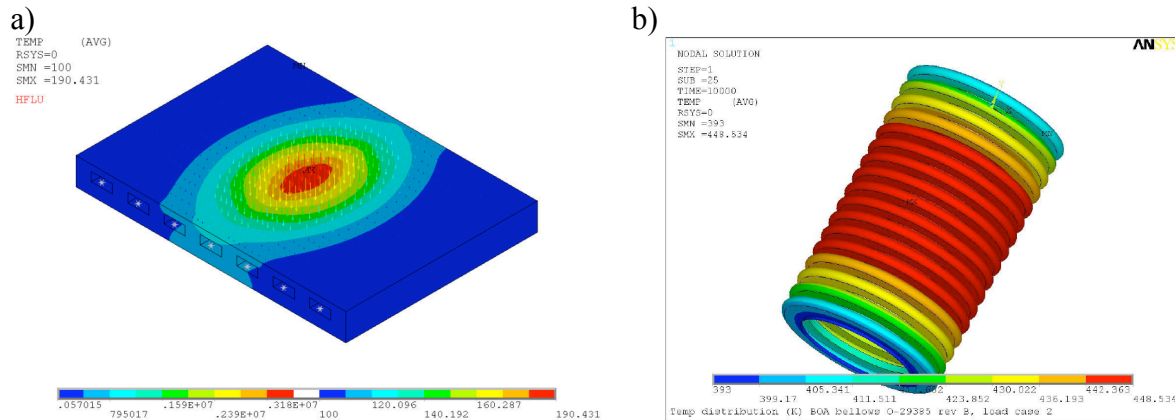


**Figure 4** The simulated temperature rise using ANSYS for a) a mitre bend mirror with 2MW incident power (peak temperature is  $\sim 190^\circ\text{C}$ ) and the bellows assuming  $0.8\text{MW/m}^3$  volumetric heating and conductively and radiatively cooled (peak temperature of  $<190^\circ\text{C}$ ).

By mid 2006 a FS launcher design had been realised that satisfied all critical design issues. This design was at a detailed conceptual design level, which is now being advanced toward a build to print design stage to be provided by the end of 2008.

**2.2 Physics Performance** The UL’s function is to stabilise the NTM. The launcher is being designed and procured by the European Union under the direction of the Close Support Unit (CSU) of EFDA. EFDA-CSU has supported the development of two launcher designs: RS and FS, with the aim of providing the optimum system based on the physics, engineering, costs, reliability, etc<sup>7</sup>. The development of the two systems was closely monitored by ITER-IT, which performed an evaluation of the two systems at the end of 2005 and chose the FS launcher as the reference design. The two systems offered equivalent operating reliability, but the FS launcher demonstrated a significant improvement in NTM stabilization efficiency ( $\eta_{\text{NTM}} = \max(j_{\text{CD}})/j_{\text{BS}}$ ) at a significantly reduced cost ( $<60\%$ ) compared to that of the RS launcher. A target value of  $\eta_{\text{NTM}} = 1.2$  was set for the UL, which should provide adequate modulated driven current inside of the island to stabilize the NTM based on a multi-machine database<sup>13</sup>. The FS launcher surpassed this target by a factor of 1.5 to nearly 3 depending on the q surface and scenario under consideration (see Table 2), thus providing adequate safety margin in case not all ECH power is available, to accommodate for errors in extrapolating to ITER, or simultaneously stabilise the q=2 and 3/2 NTMS.

**TABLE 2. Comparison of the RS and FS launchers capabilities in stabilizing the NTMs,  $\eta_{\text{NTM}}$  values are given for the three ITER scenarios based on the calculated  $j_{\text{CD}}^1$  values using GRAY<sup>14</sup>.**

	Scenario 2		Scenario 3a		Scenario 5	
	q=3/2	q=2	q=3/2	q=2	q=3/2	q=2
RS Launcher <sup>4</sup>	0.56	1.27	0.36	0.69	0.53	0.91
FS Launcher <sup>5</sup>	2.52	3.54	1.82	2.69	1.93	2.07
Relative difference	4.5	2.8	5.1	3.9	3.6	2.3

**3 Synergetic Launcher Design** The upper port launcher has the sole function of stabilising the NTMs, while the equatorial port launcher has to perform all other functions (sawtooth control,

assist in L to H-mode transition, central heating, current profile control). The partitioning of the physics tasks is somewhat imbalanced with one single equatorial port required to perform several tasks and four upper ports devoted to a single task. Some of the tasks designated for the EL require a large driven current fraction (useful for current profile tailoring), while others require a narrow deposition profile (useful for sawtooth control). Designing an EL that can achieve both of these tasks in the ITER environment is not realistic. For example, the present EL is inadequate for sawtooth control in the region of  $0.4 \leq \rho_p \leq 0.65$  and does not provide access with the full power inside of  $\rho_p < 0.3$ , as shown by the red zones in figure 5 centre image.

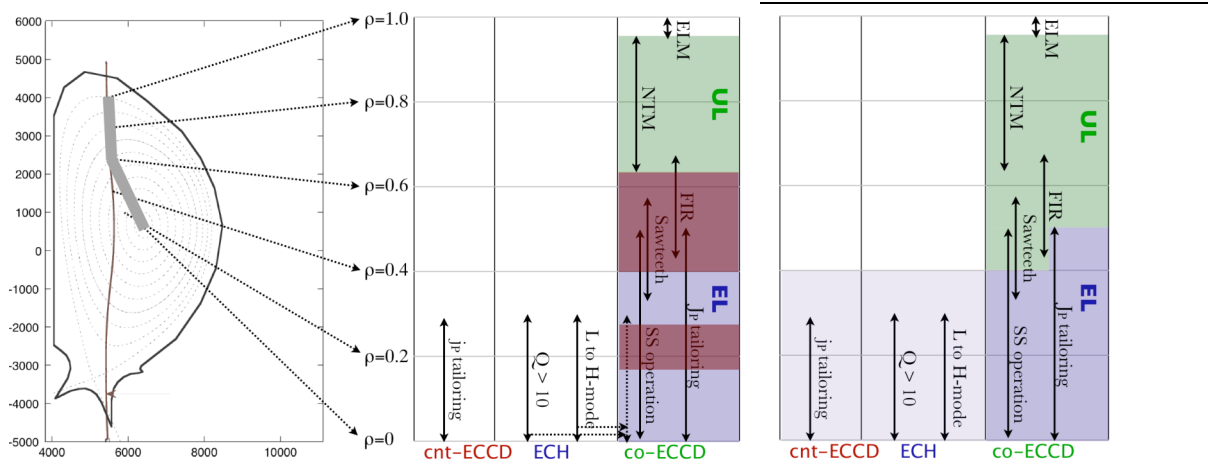


**Figure 5.** The EC capabilities of the two launcher ITER system based on the present capabilities (center) with the dark bands representing limited performance or access from the EL, and (right) from the synergetic design proposed in this paper and reference [15].

Therefore, the partitioning of the EC applications have been reinvestigated looking at a division based on the characteristics of the two launchers<sup>15</sup> for a more synergetic approach. The EL steers the beam in the toroidal direction resulting in relatively large driven current fractions and broad deposition profiles, while the UL steers the beams in the poloidal direction with a fixed toroidal angle optimised for a narrow and peaked current density deposition profile. Thus there is a natural division of the EC functions between the two launchers: EL applied when either a large current fraction or central deposition is needed and the UL applied when a narrow-peaked current density profile is needed. Such a redistribution would require the UL to access up to  $\rho_p \sim 0.4$  as shown in figure 5 right image. This would relax the steering requirement on the EL, which could then be modified to provide some counter-ECCD capabilities useful for additional current profile tailoring and providing pure ECH by balancing the co and counter-ECCD contributions thus decoupling the current and heating aspects. The following sections describe how each launcher could be modified to achieve the synergetic ECH system. Note that the present reference design of the UL is the Extended Performance Launcher (EPL) design, which includes the modifications described below.

**3.1 Modifications to the upper launcher** In the present ITER port configuration, the four upper ports are devoted to the upper launcher, which implies a total of 32 entries for the 24 ECH available beam lines. The eight additional entries could have been used as a spare system in case of steering mechanism failure in one of the other ports. Instead, the eight entries are to be used to modify scanning range of the launcher to extend the physics performance, while reducing the engineering constraints on the steering mechanism. This later option, referred to as Extended Performance Launcher (EPL), offers an optimisation of both the launcher's engineering and physics performance and can be achieved simply by spreading out the deposition range of the two steering mirrors as illustrated in Figure 6. The upper steering mirror (USM) aims further inward covering the range of  $0.4 \leq \rho_p \leq \sim 0.88$ , reaching the  $q=1$  surface to provide access for sawteeth control. The lower steering mirror (LSM) covers the outer region of the plasma over the range of  $0.75 \leq \rho_p \leq 0.93$ . Spreading the two steering ranges out results in three zones: upper ( $\sim 0.88 \leq \rho_p \leq 0.93$ ) and lower ( $0.4 \leq \rho_p \leq \sim 0.75$ ) zones accessible with 16 beams (or 13.3MW) and a middle zone where the USM and LSM overlap ( $\sim 0.75 \leq \rho_p \leq \sim 0.88$ ) accessible with the full 20MW. Note that a switching system will be required prior

to the entrance to the port plug to deviate the power to either the USM or LSM depending on the physics requirements.

The EPL design has a far reaching impact. First, the overall rotation of each steering mirror is reduced from  $\pm 6.5^\circ$  to  $\pm 5.5^\circ$ . The reduction of  $\pm 1^\circ$  nearly doubles the number of cycles prior to the onset of fatigue (as seen in figure 3b). Second, the opening in the front wall panel is smaller, reducing the nuclear radiation on the steering mechanism. Third, the increased access region implies that the EC power can be more effective in controlling the sawtooth instability when launched from the upper port thus extending the physics performance of the EC system<sup>15,16</sup>. Finally, as will be discussed in the following section, the steering requirements on the equatorial launcher can be relaxed impacting both the EL's engineering constraints and physics requirements.

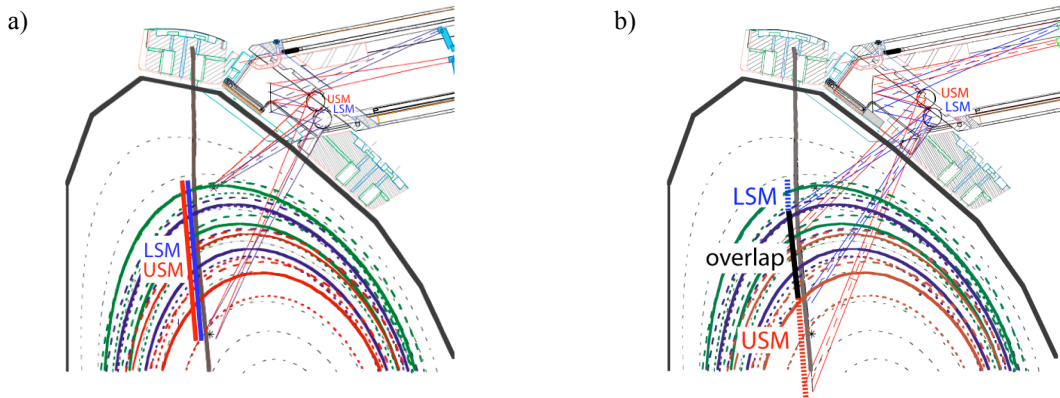


**Figure 6** (a) The NTM launcher limits both LSM and USM to provide access over the region in which NTMs are expected to occur. (b) The extended performance launcher (EPL) shifts the deposition of the USM to access further inward for an enhanced physics programme.

**3.2 Modifications to the equatorial launcher** Using the extended physics launcher as described above would alleviate the large steering requirements on the EL ( $0.0 \leq \rho_\psi \leq 0.65$ ) such that the EL would only have to access  $0.0 \leq \rho_p \leq 0.5$  thus reducing the steering range to  $20^\circ \leq \beta \leq 37^\circ$ . Note that beyond  $\rho_p > 0.55$  the beams are not fully absorbed resulting in large amounts of power passing through the plasma toward neighboring diagnostic ports<sup>16</sup>. There is also a limited power accessible inside of  $\rho_p \leq 0.3$  arising from the horizontal steering plane of the top and bottom beam assemblies offset from the plasma center, this could be avoided by adding a small tilt of these beam assemblies such that the steering plane intersects the plasma center.

Reducing the steering range requires a smaller opening in the BSM (see figure 7a), decreasing the radiation impact on the EL steering mechanism. Note that the steering mechanism in the EL is more susceptible to nuclear heating and damage than in the UL due to the proximity and direct line of sight to the plasma core, reducing the opening in the front wall offers better protection for the steering mechanism.

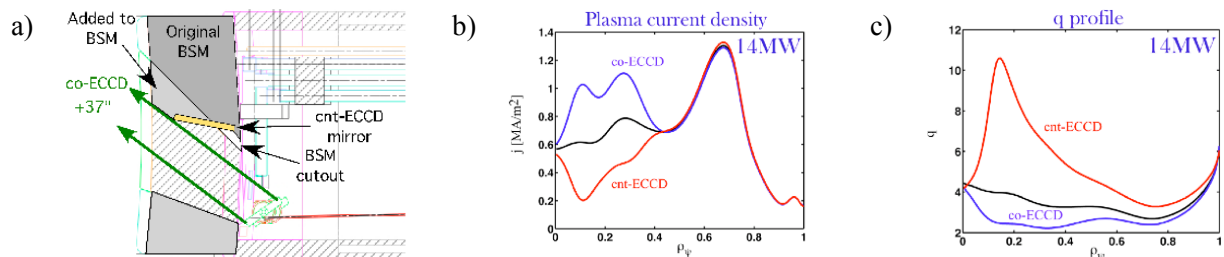


**FIGURE 7.** a) EL design with counter ECCD using an additional mirror in BSM. Modifications of b) current profile and c) q-profile using co or cnt-ECCD in scenario.

The EL could be modified to provide cnt-ECCD by including a fixed mirror in the BSM region as illustrated in Figure 7a. To change from co to cnt-ECCD the ECH beam would be turned off, the steering mirror rotated to aim at the additional mirror and then the ECH beam turned back on again with the beam reflected in the counter direction. The mirror curvature, tilt angle and size can be

chosen for optimum deposition region and profile in the cnt-ECCD direction. This modification can be made to all three steering rows providing the full range from 20MW in co-ECCD to 20MW in cnt-ECCD with a switching time of  $\sim 1$ sec. Note that the steering range would increase slightly from  $\Delta\beta=25^\circ$  to  $\sim 32^\circ$  (depending on desired functionality, design optimisation and engineering limitations of the steering mechanism).

In addition to the possibility of providing independent control of the heating and current drive contribution, cnt-ECCD can also be used to control the degree of negative shear in the internal transport barrier (ITB). For example, in Figure 7b, 14MW of co or cnt-ECCD is applied centrally to either fill-in or deepen the hollow current profile of scenario 4, which results in either a flattening or more reversed q-profile (as shown in Figure 7c). This provides a mechanism for optimizing the ITB performance, controlling both  $q_0$  and  $q_{\min}$  and avoiding the onset of ideal MHD modes that can occur near rational values of  $q_{\min}$  or too steep of pressure profiles.

**4. Conclusions and Acknowledgements** Solutions to all of the critical issues related to installing an FS launcher in the ITER upper port have been realized. In particular, a frictionless backlash free steering mechanism has been developed that satisfies the cyclic requirements needed to stabilize the NTMs during the full lifetime of ITER and is also compatible with the EPL design.

The present ITER ECH system has a strong imbalance in the partitioning of functions, with the UL responsible for only NTM stabilization and the EL for all other applications requiring twice the access range as compared to the UL. The EL is also required to perform applications that require a large driven current (current profile control, bulk current drive, etc.) and narrow deposition profile (sawtooth control), which are difficult to accomplish within the physical limitations of the launcher (scanning range, port size, BSM opening, etc.). As a result the ECH system has limited performance in applications such as sawtooth control and current profile tailoring. An alternative partitioning of the physics applications has been proposed that partitions the applications based on the strengths of each launcher system: EL offering larger driven current and central deposition and UL offering a narrow deposition profile. Modifications to both launchers are proposed to achieve this synergetic approach, while simultaneously relaxing the engineering constraints on both launchers.

This work, supported by the Swiss National Science Foundation and the European Communities, was carried out within the framework of the European Fusion Development Agreement (ECHULA subtask (f) /contract EFDA TCP 341-22 and ECHULB subtask (b) /contract EFDA 05-1228). The views and opinions expressed herein do not necessarily reflect those of the European Commission.

## References

- <sup>1</sup> J. How, P. Barabaschi, W. Spears Project Integration Document, G A0 GDRD 6 04-09-09 R0.2.
- <sup>2</sup> K. Takahashi *et al*, Fusion Science and Technology **47** (2005) p1.
- <sup>3</sup> G. Ramponi *et al*, Journal of Physics: Conference Series **25** (2005) ) 243-251.
- <sup>4</sup> C.P. Moeller *et al*, A method of remotely steering a microwave beam launched from a highly overmoded corrugated waveguide Proc. 23<sup>rd</sup> Int. Conf. on IRMMW (1998) p.1487-1500.
- <sup>5</sup> T. Verhoeven *et al*, Journal of Physics: Conference Series **25** (2005) 84-91.
- <sup>6</sup> M.A. Henderson *et al*, Journal of Physics: Conference Series **25** (2005) 143-150.
- <sup>7</sup> R. Heidinger *et al*, this conference IT-P2/10.
- <sup>8</sup> G. Saibene *et al*, this conference IT-P2/14.
- <sup>9</sup> R. Chavan *et al*, Journal of Physics: Conference Series **25** (2005) 151-158.
- <sup>10</sup> J.-D.Landis *et al*, Submitted Fusion Engineering Design.
- <sup>11</sup> Expansion Joint Manufacturers Association, Inc., 25 North Broadway, Tarrytown, New York 10591
- <sup>12</sup> ITER Tech Basis, <http://www.iter.org/pdfs/PDD2-5.pdf>.
- <sup>13</sup> RJ La Haye *et al*, Nucl Fus **46**(2006) 451.
- <sup>14</sup> D. Farina *et al*, submitted for publication in Fus Science and Tech. Special Issue on ECH..
- <sup>15</sup> M.A. Henderson *et al*, *The ITER ECH FS launcher Design for an Optimized Physics performance*, 14<sup>th</sup> Workshop on ECE and ECRH, Santorini, Greece May, 2006.
- <sup>16</sup> G. Ramponi *et al*, accepted for publication in Fus Science and Tech. Special Issue on ECH.